

## Abstract

The high rate of attrition among clinical-stage therapies highlights the need for *in vitro* models that generate data which translates into the clinic. Fully human bioprinted tissues with spatially-controlled architecture enable biochemical, genetic, and histologic interrogation following exposure to modulators of interest, making them valuable *in vitro* tools for toxicology and disease modeling. We have generated bioprinted human liver tissues exhibiting histological and functional similarity to native liver, with sustained viability (ATP, albumin) and CYP3A4 activity over 4 weeks. The liver tissues display hallmark biochemical and histologic responses to hepatotoxicants such as valproic acid, exemplified by decreases in ATP and GSH and the accumulation of cytoplasmic vacuoles within the hepatocytes reflective of a steatotic disease phenotype. Characterization of bioprinted human tissues that mimic the kidney proximal tubule reveal a well-organized tubulointerstitial interface, with CD31+ endothelial cell networks throughout the interstitium, formation of a polarized layer of renal epithelium on top of the interstitium, and a basal lamina. Finally, a tissue model for the breast tumor microenvironment has been developed to better predict drug efficacy on both cancer cells and the surrounding stroma.

## Introduction

- Cells reside in heterogeneous and architecturally structured 3D environments *in vivo*
- Using the proprietary NovoGen Bioprinter<sup>®</sup> Platform, Organovo builds 3D tissues through automated, spatially-controlled cellular deposition to better recapitulate native tissue structure and function.

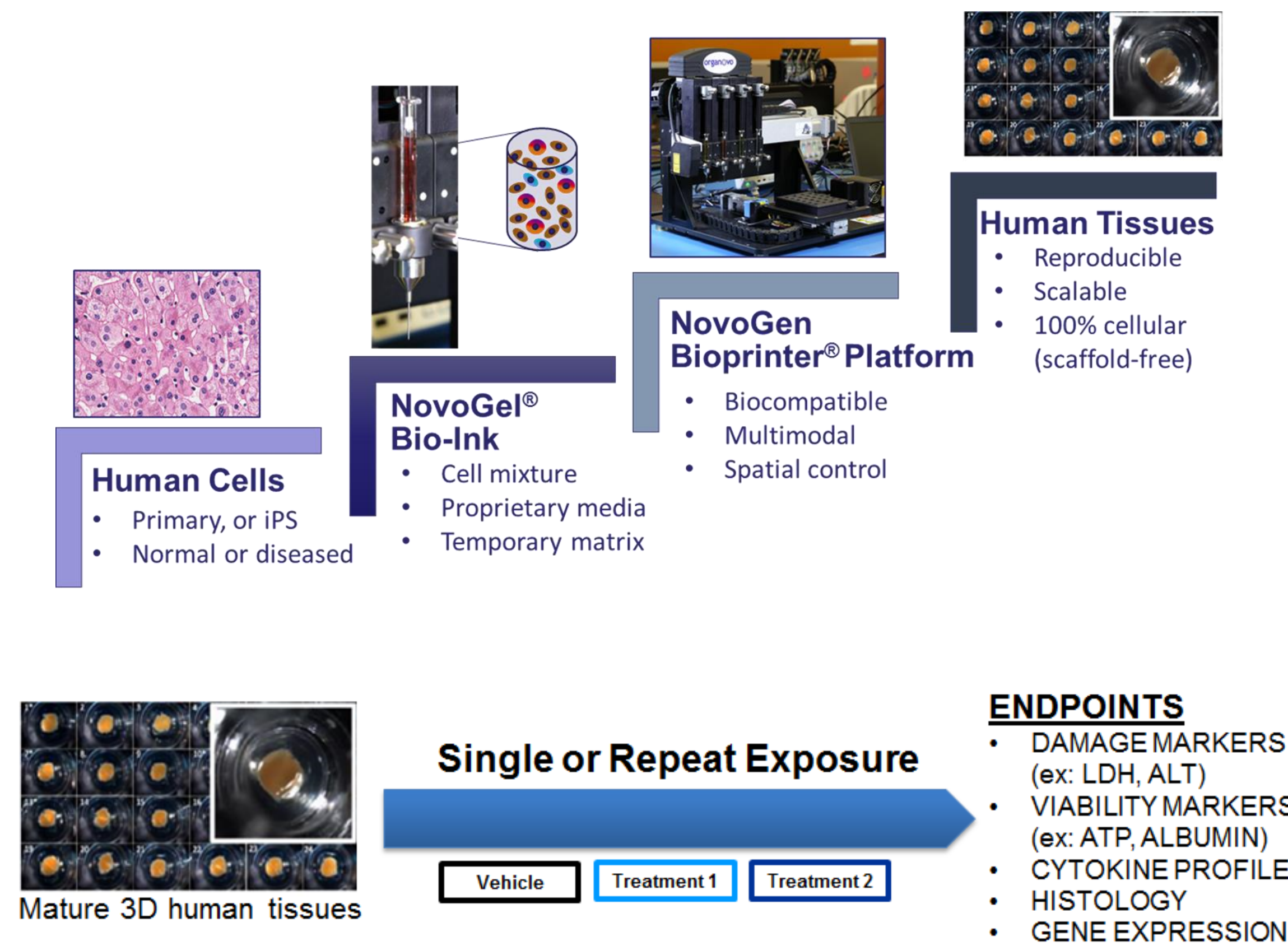


Figure 1: 3D human tissue development using the NovoGen Bioprinter<sup>®</sup> Platform, and a sample experimental workflow.

## 3D Kidney Proximal Tubule tissues model nephrotoxicity

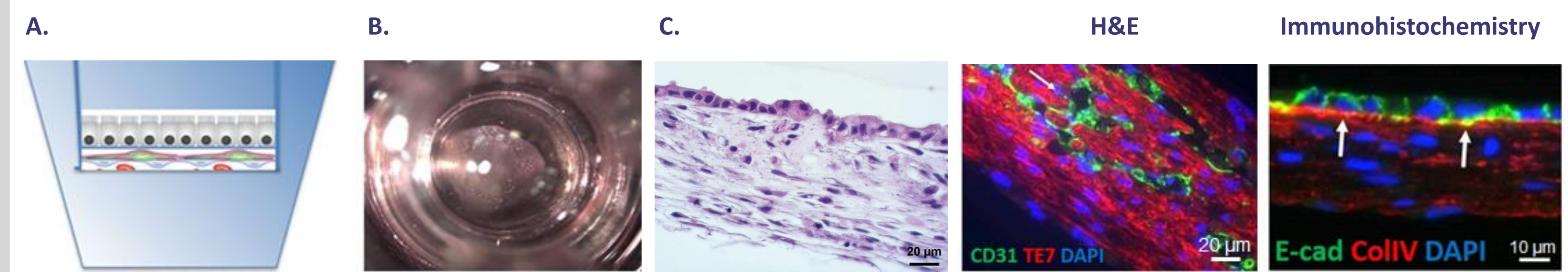


Figure 5: Schematic (A) and macroscopic view (B) of 3D bioprinted human proximal tubule tissues comprising renal fibroblasts, HUVEC, and RPTCC. (C) Histological characterization shows robust CD31<sup>+</sup> endothelial networks, TE7<sup>+</sup> fibroblasts, E-cadherin (E-cad) epithelial junctions, and a collagen IV (ColIV) basal lamina.

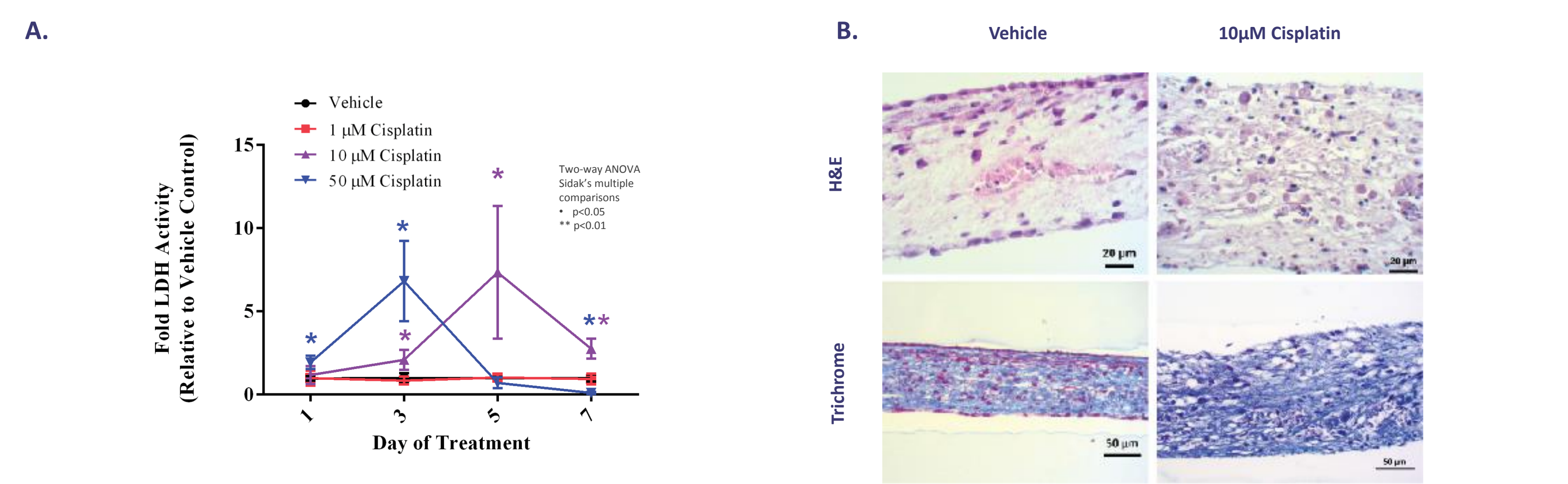


Figure 6: (A) 3D proximal tubule tissues demonstrate an increase in damage marker LDH following Cisplatin treatment. (B) H&E and Trichrome analysis show a loss of epithelial cells, increased tissue thickness, and fibrosis following Cisplatin treatment

## exVive3D<sup>™</sup> Liver tissues model clinically relevant toxic phenotypes

### Tissue Characterization

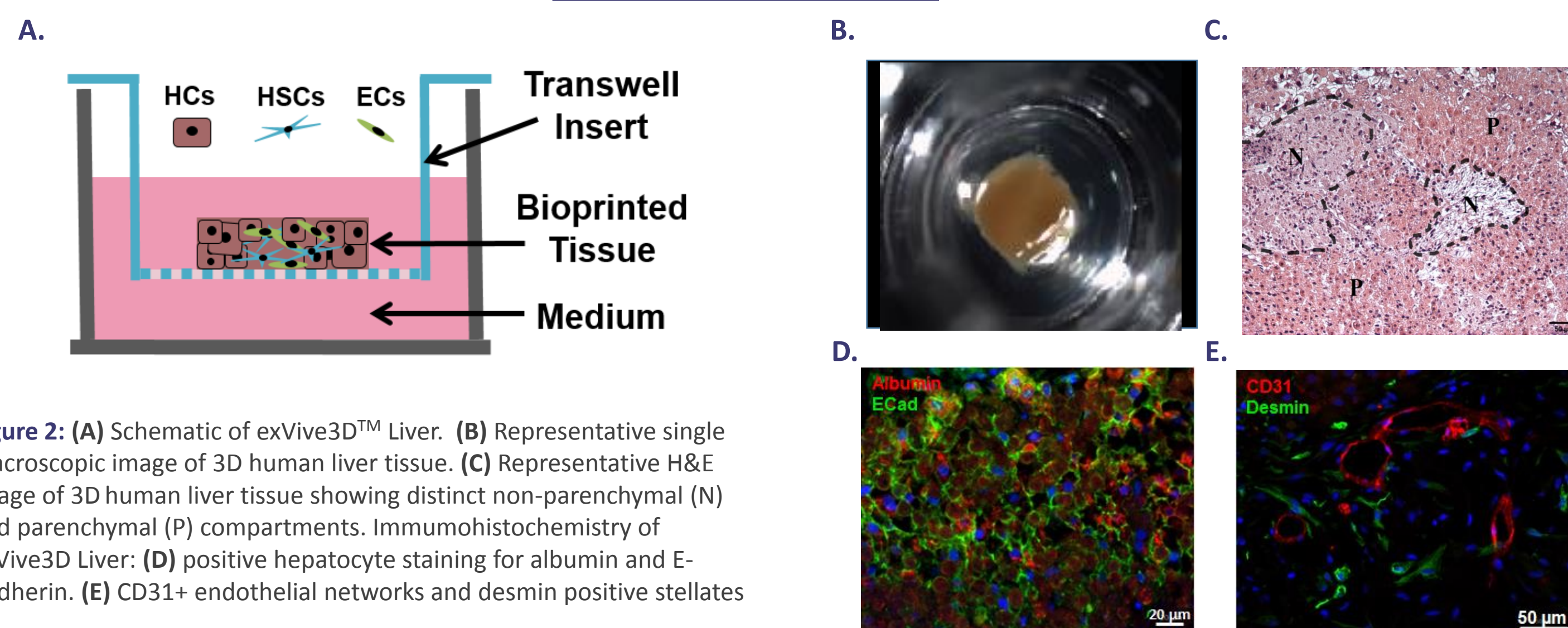


Figure 2: (A) Schematic of exVive3D Liver. (B) Representative single macroscopic image of 3D human liver tissue. (C) Representative H&E image of 3D human liver tissue showing distinct non-parenchymal (N) and parenchymal (P) compartments. Immunohistochemistry of exVive3D Liver: (D) positive hepatocyte staining for albumin and E-Cadherin. (E) CD31<sup>+</sup> endothelial networks and desmin positive stellates

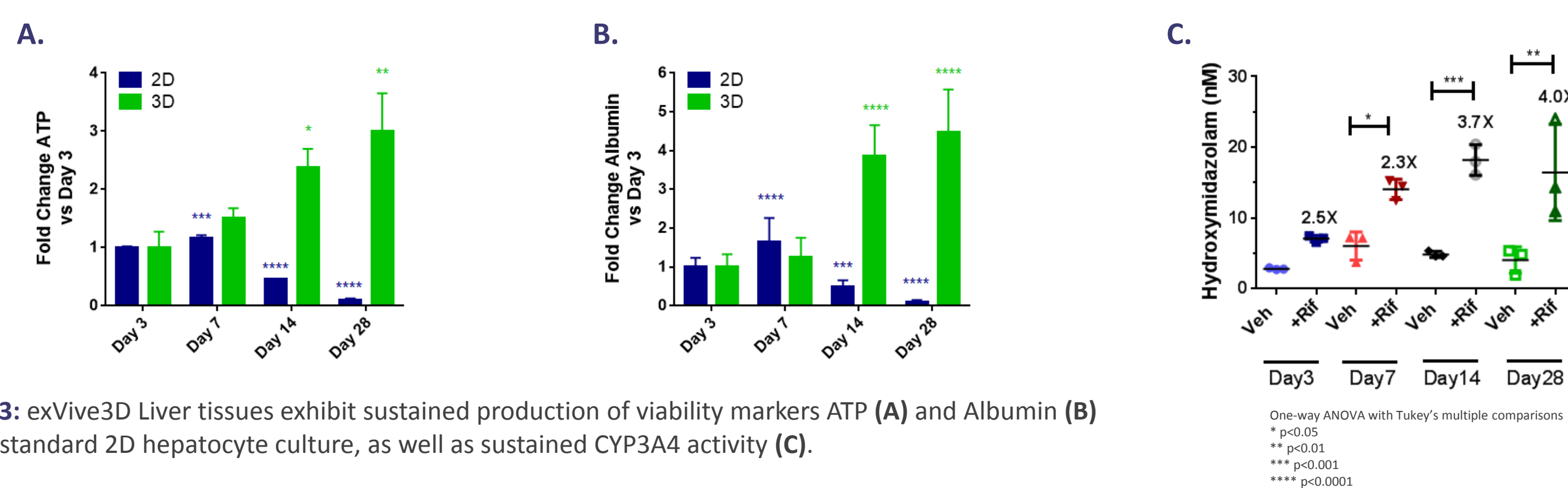
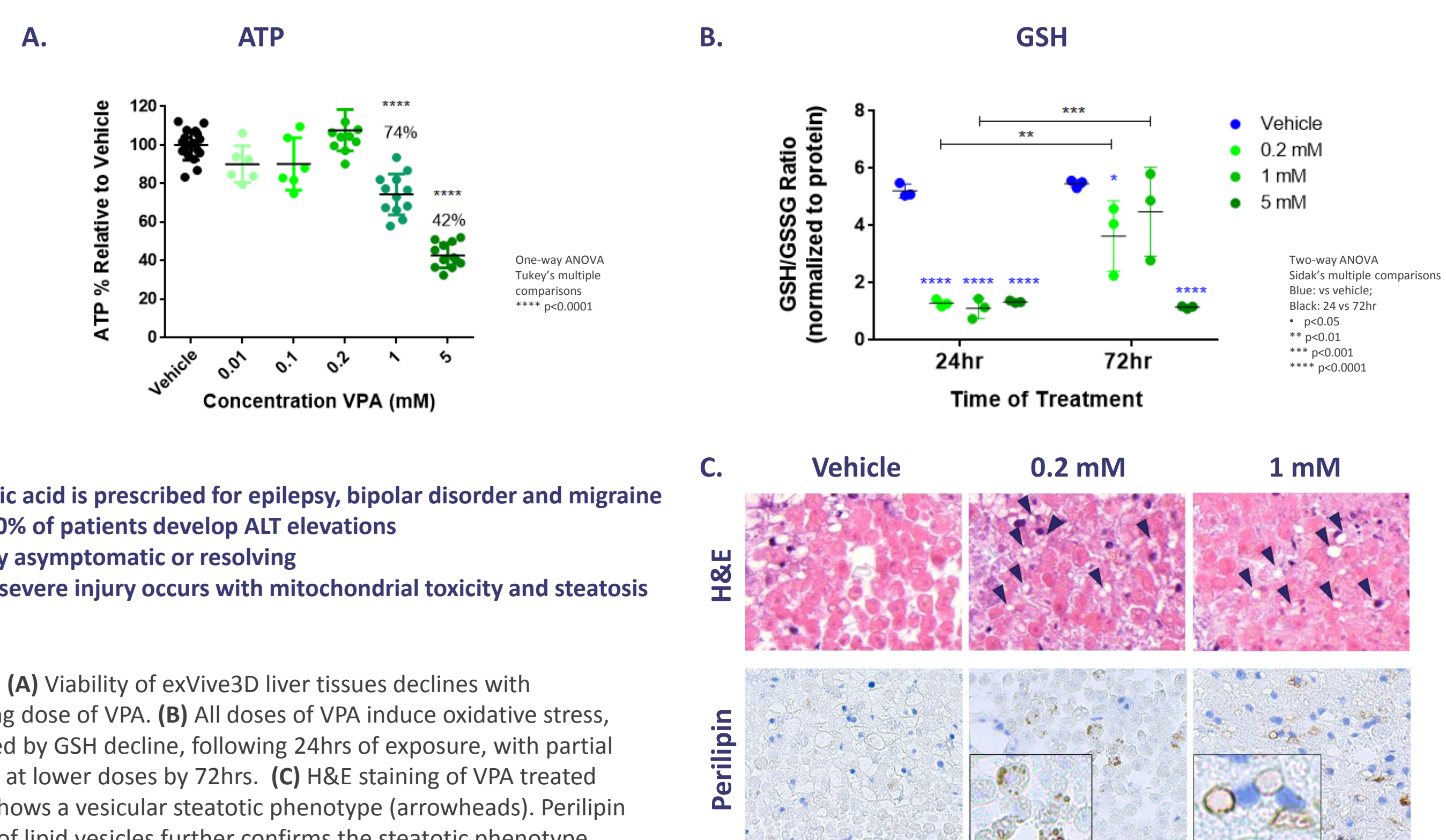


Figure 3: exVive3D Liver tissues exhibit sustained production of viability markers ATP (A) and Albumin (B) versus standard 2D hepatocyte culture, as well as sustained CYP3A4 activity (C).

### Valproic Acid Induced Steatosis



- Valproic acid is prescribed for epilepsy, bipolar disorder and migraine
- 5% - 10% of patients develop ALT elevations
- Usually asymptomatic or resolving
- Rarer, severe injury occurs with mitochondrial toxicity and steatosis

Figure 4: (A) Viability of exVive3D liver tissues declines with increasing dose of VPA. (B) All doses of VPA induce oxidative stress, evidenced by GSH decline, following 24hrs of exposure, with partial recovery at lower doses by 72hrs. (C) H&E staining of VPA treated tissues shows a vesicular steatotic phenotype (arrowheads). Perilipin staining of lipid vesicles further confirms the steatotic phenotype.

## Tumor Microenvironment Model

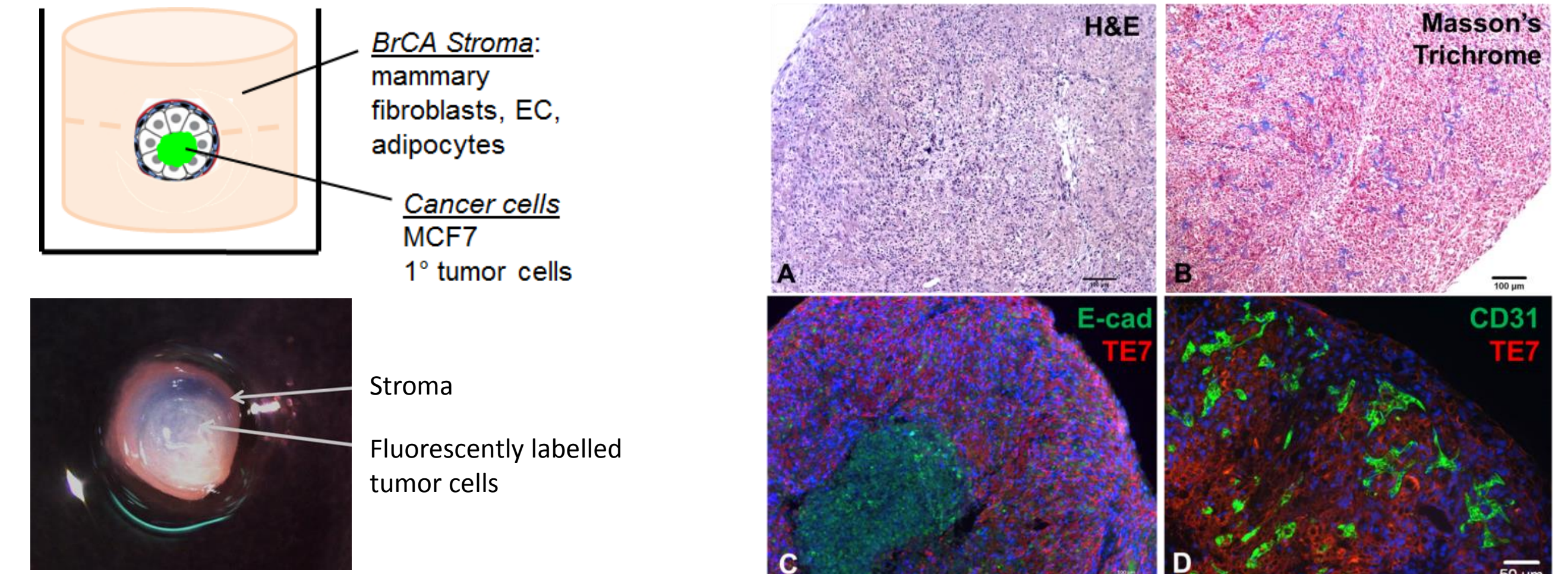


Figure 7: Left, Top: Schematic of bioprinted tissues. A nodule of human breast cancer cells is surrounded by a stromal compartment composed of endothelial cells, fibroblasts, and adipocytes. Bottom: Bioprinted tissues immediately after printing. Cancer cells are labeled with blue dye. Right: Histological analysis of bioprinted tissues. (A) Hematoxylin and eosin stain. (B) Masson's Trichrome stain. Collagen is indicated by blue staining. (C) E-cadherin (green) and TE7 (red) staining marks cancer cells and fibroblasts, respectively. (D) CD31 (green) staining indicates areas of microvasculature formation in the stromal compartment containing fibroblasts (TE7, red).

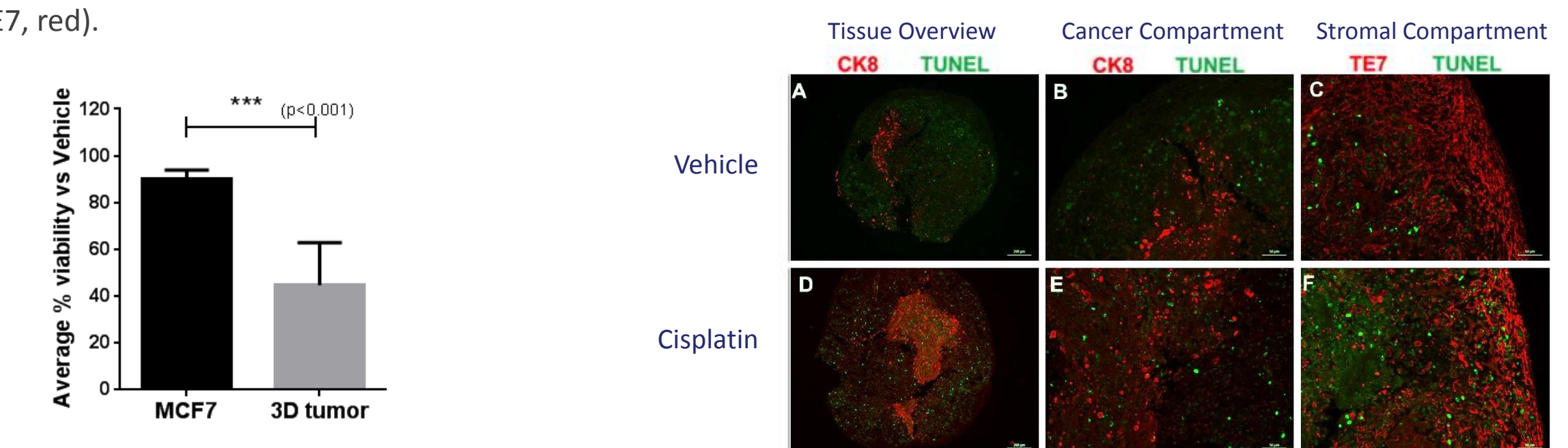


Figure 8 Left: MCF7 cells alone or bioprinted tissues were treated with 100 uM cisplatin for 48 h (MCF7) or daily for 4 days (bioprinted tissues) and assessed for viability by CellTiter Glo. Right: Bioprinted tissues were treated with vehicle (A-C) or 100 uM cisplatin (D-F) for 4 days and assessed for apoptosis by TUNEL staining (green) and markers for cancer cells (red; A, B, D, E) or fibroblasts (C, F). Cisplatin induces greater apoptosis in the stromal compartment than in the cancer compartment.

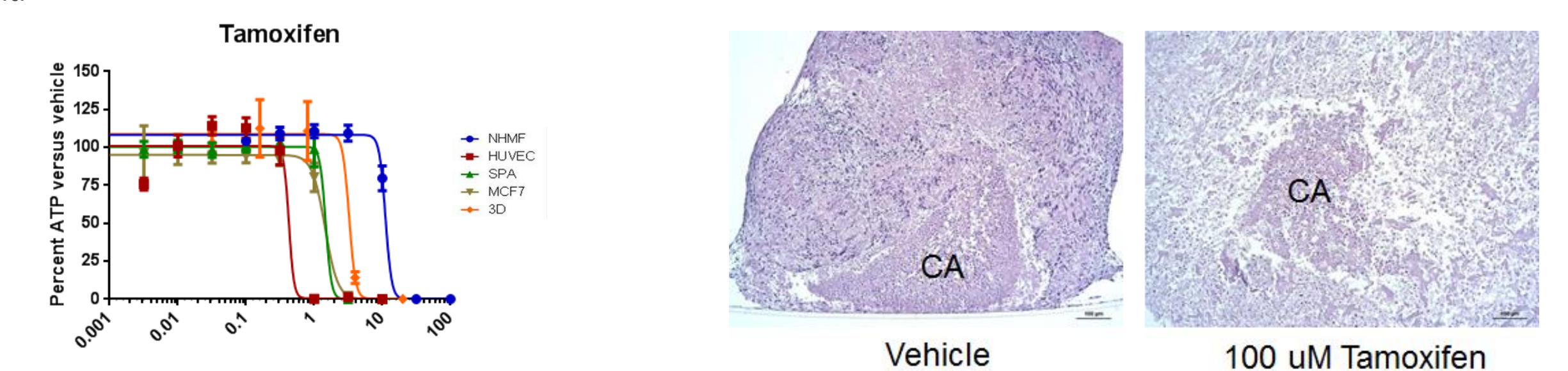


Figure 9 Differential sensitivity seen between component cells cultured in 2D and 3D bioprinted tissues. Left: Dose response curves for tamoxifen treated 2D cell cultures vs. 3D bioprinted tissue model. Right: Histological assessment of effects of tamoxifen on stroma and cancer (CA) compartments.

## Summary

- Recapitulating native physiology *in vitro* requires an appreciation of cell, tissue, and organismal context
- Organovo's bioprinting platform enables the construction of architecturally correct 3D human tissues through controlled cellular placement without the use of exogenous scaffolding
- The biological complexity of the bioprinted tissues allows the end user to model multi-factorial toxicological and disease processes